Published by
NIGERIAN SOCIETY OF PHYSICAL SCIENCES
Available online @ https://asr.nsps.org.ng/index.php/asr

African Scientific Reports 5 (2026) 367

African Scientific Reports

Efficient and optimal adsorptive removal of urea from agricultural effluent using acidified ball clay: optimization via response surface methodology

E. A. Yerima[a,e,*], S. P. Maaji[a,b], C. V. Ogbodo[c], D. Abutu[d], S. A. Yakubu[e], F. O. Nwankwo[a], S. J. Aboki[a], J. A. Adamu[a]

[a]*Department of Chemistry, Federal University Wukari, PMB 1020, Taraba State, Nigeria*
[b]*Department of Chemistry and Biochemistry, Auburn University, Alabama, USA*
[c]*Department of Chemistry, National Open University of Nigeria, Abuja, Nigeria*
[d]*Department of Chemical Engineering, Faculty of Engineering, Federal University Wukari, PMB 1020, Taraba State, Nigeria*
[e]*Department of Chemistry, University of Jos, PMB 2084, Plateau State, Nigeria*

Abstract

Agricultural runoff rich in urea content poses a threat to the aquatic ecosystems. This study investigated the adsorptive potential of acidified ball clay in removing urea from agricultural effluents as well as the conditions of temperature, adsorbent dosage, time, and pH that will give the optimum removal by adopting response surface methodology (RSM). Characterizations of the acidified ball to understand its adsorptive properties revealed the abundance of visible pores on the acidified ball clay for possible accommodation of adsorbate (urea) by SEM, while after adsorption the initial visible pores are slightly batched, indicating interaction between the adsorbate and adsorbent. The TEM analysis showed a number of spherical-shaped and well-dispersed nanostructures of adsorbent whose number doubles on addition of adsorbate after adsorption. The FTIR spectrum of modified ball clay showed the presence of O-H, Si-O-Si, and Al-OH groups. The EDX spectrum for the acidified ball clay unveils the elemental composition by weight in the order: Si (59.0%) > Al (18.4%) > O (12.3%) > N (3.0%) = C (3.0%) > Fe (2.8%) > Ca (1.3%). The batch process showed that acidified ball clay exhibited good potential for urea adsorption. Achieving a maximum removal efficiency of 89.14% with a corresponding capacity of 1815.3 mg/g from an initial concentration of 152.7 mg/L at optimum conditions of pH = 3, temperature = 35°C, dosage 3.75 g, contact time = 30 minutes, and rate of 4.53 min^{-1}.

DOI:10.46481/asr.2026.5.1.367

Keywords: Acid modified, Ball clay, Characterization, Contamination, Remediation

Article History :
Received: 26 September 2025
Received in revised form: 27 November 2025
Accepted for publication: 03 December 2025
Published: 10 February 2026

© 2026 The Author(s). Published by the Nigerian Society of Physical Sciences under the terms of the Creative Commons Attribution 4.0 International license. Further distribution of this work must maintain attribution to the author(s) and the published article's title, journal citation, and DOI.

1. Introduction

Agricultural inputs such as urea fertilizers play an important role in meeting the world's growing food demands. However, their use can generate significant environmental challenges if not managed sustainably. For instance, the discharge of agricultural

*Corresponding author: Tel. No: +234-803-750-1512.
Email address: yerimaemmanuel@yahoo.com (E. A. Yerima)

effluents into water bodies may lead to the contamination of natural water resources [1, 2]. Agricultural effluents comprise runoff and wastewater generated from activities such as irrigation, fertilization, and pesticide application, carrying various pollutants and contaminants. When these effluents reach water bodies such as rivers, lakes, or groundwater, they pose serious environmental risks. These effluents often contain pollutants such as excess nutrients: urea, phosphate, and nitrate that can have detrimental effects on aquatic ecosystems. High concentrations of urea in water bodies can lead to eutrophication, a process characterized by excessive algae and aquatic plant growth. This overgrowth depletes oxygen levels, disrupts aquatic ecosystems, and can cause blockages in pipes when such effluents are discharged [3–5].

The use of pesticides to control pests and diseases in crops can also contribute to agricultural effluents. These chemicals may be washed off from fields during rainfall or irrigation, contaminating water sources and potentially harming non-target organisms. Additionally, livestock farming produces effluents in the form of animal waste and excess feed, which can contaminate nearby water sources. The high organic matter and nutrient content in livestock waste can lead to water pollution if not properly managed. To address urea contamination in agricultural effluents, various treatment methods have been developed. Biological treatments, including natural biodegradation in aerobic continuous flow systems, microbial remediation, fluidized bed reactors, and wetlands, have been explored. Chemical treatments such as adsorption, photocatalytic degradation, and electrochemical methods have also been investigated [6, 7]. Among these, adsorption has emerged as a promising approach due to its efficiency, cost-effectiveness, and ability to selectively remove specific contaminants.

Previous studies have shown that ball clay a type of kaolin clay ($Al_2O_3{\cdot}2SiO_2{\cdot}2H_2O$) possesses excellent adsorption properties, plasticity, dry strength, and shrinkage. It has been used in wastewater treatment, air purification, and as a catalyst support in heterogeneous catalysis. Additionally, ball clay is employed as a bleaching agent in the refining of oils, fats, and waxes. Its acid-activated structure aids in removing unwanted pigments and contaminants, thereby improving the appearance and quality of final products. It also serves as a soil conditioner, enhancing soil structure and nutrient retention. The clay's water-holding capacity and cation exchange capacity make it beneficial for soil amendment in agricultural practices. Furthermore, ball clay can function as a filler or extender, improving the rheological properties of various products [8, 9].

As a material composed mainly of kaolinite and other minerals, ball clay's high surface area and porous structure suggest its potential as an adsorbent for removing pollutants from water [10]. To optimize the removal of urea using ball clay, several parameters must be considered, including urea concentration, pH, temperature, adsorbent dosage, and contact time [11]. Response Surface Methodology (RSM), a statistical technique that models and optimizes multiple variables simultaneously, can be employed to determine the optimal conditions for maximum urea adsorption while minimizing resource use and experimental time [12–14].

This study aims to address urea contamination in agricultural effluents by exploring the use of ball clay as an adsorbent for urea removal. It also seeks to identify the optimal conditions: such as pH, temperature, adsorbent dosage, and contact time for achieving maximum adsorption efficiency. The findings are expected to provide valuable insights into the adsorption mechanisms of urea onto ball clay and to establish a comprehensive understanding of the conditions necessary for optimal removal. Ultimately, this research aims to contribute to the development of a sustainable and effective approach for treating agricultural effluents, reducing urea pollution, and mitigating eutrophication's impact on water ecosystems.

2. Material and methods

The experimental design was conducted using "Design Expert version 13," which recommends 29 batches of experimental runs at varying temperatures (25–45°C), ball clay dosages (1.5–6.0 g), pH levels (3–11), and contact times (30–90 minutes), based on insights from previous studies [9].

2.1. Sample collection

The ball clay used in this work was supplied by Central Drug House (P) Ltd., located at 7/28 Vardaan, Daryaganj, New Delhi - 110002, India. The ball clay was spherical in shape, grey in color, with a kaolinite content of approximately 75%. The agricultural effluents, containing moderate amounts of urea, were collected using pre-cleaned containers from three locations within the geographical coordinates: 7.216051N, 9.574020E; 7.215463N, 9.571065E; and 7.214531N, 9.569122E. These samples were collected around a rice farm located in Harga, Kastina-Ala, Benue State, Nigeria, using stratified sampling. The water samples were homogenized to produce a composite sample.

2.2. Sample preparation and modification

The ball clay was crushed into powder and passed through a 5 μm mesh sieve. Subsequently, 80 g of the clay powder was oven-dried at 100°C for 3 hours to remove moisture. To 70 g of the dried clay in a 125 mL Erlenmeyer flask, 700 mL of 0.1 M H_2SO_4 was added. The mixture was heated under reflux at 100°C with magnetic stirring at 400 rpm for 6 hours. Afterward, it was allowed to stand for 30 minutes, then rinsed repeatedly with deionized water to remove leachable impurities. The resulting product was dried in an incubator at 60°C for 6 hours, cooled, pulverized, and labeled as Modified Ball Clay (MBC) [15, 16].

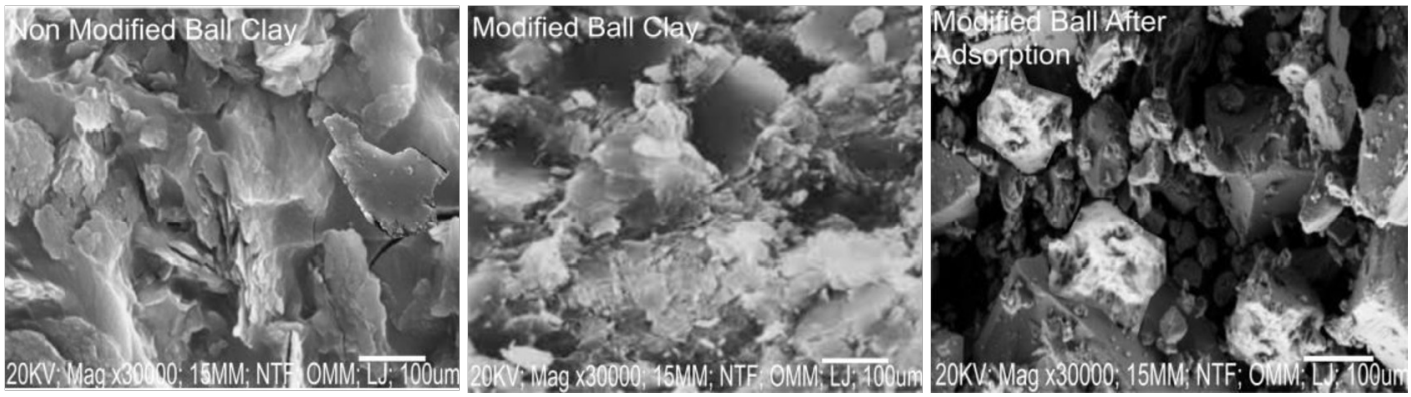


Figure 1. Scanning electronic micrograph of non-modified, modified and modified ball clay after adsorption at 100 μm magnification.

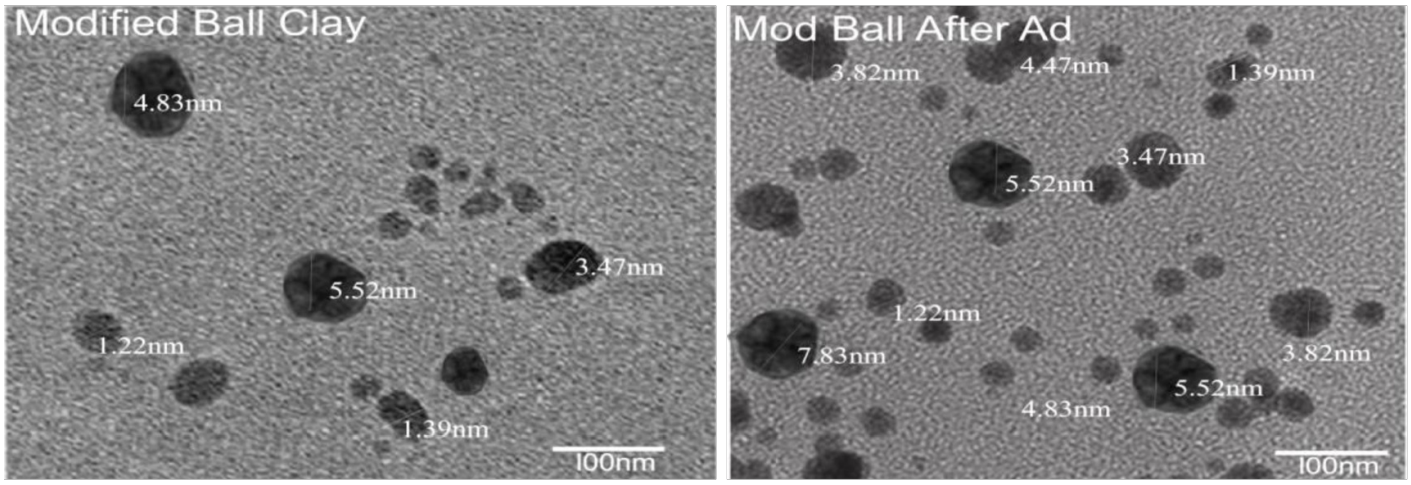


Figure 2. Transmission electron micrograph of modified ball clay before and after adsorption at 100 nm magnification.

2.3. Characterization of acid-modified ball clay

The surface morphology of the modified ball clay was examined using a Scanning Electron Microscope (JOEL JSM 7600F) and Transmission Electron Microscope (TEM). Functional groups embedded in the adsorbent were identified using a Fourier Transform Infrared (FTIR) spectrophotometer (Nicolet iS10). Elemental composition was analyzed with an Energy Dispersive X-ray (EDX) spectrometer [17].

2.4. Batch experimental design and procedure

The batch adsorption experiments were designed using Response Surface Methodology (RSM) implemented in Design Expert (version 13) software. A Box–Behnken Design (BBD) was employed to evaluate the combined effects of key process variables on urea removal by the MBC adsorbent [18]. The design generated 29 experimental runs, each representing a unique combination of the independent variables, as shown in Table 1.

For the first run, 1.5 g of MBC was accurately weighed and transferred into a 250 mL Erlenmeyer flask containing 50 mL of agricultural effluent with an initial urea concentration of 152.7 mg/L. The pH of the solution was adjusted to the desired level (pH 11) using 0.1 M HCl and 0.1 M NaOH, with pH monitored via a pH meter (Model Starter 2100). The mixture was then equilibrated in a water bath (Model Clifton 98006) maintained at 35°C to ensure uniform temperature distribution before agitation.

Adsorption was carried out using a cycling vibrator (Model HY-4) at a controlled shaking rate for 60 minutes, ensuring adequate interaction between urea molecules and the MBC adsorbent. After agitation, the samples were filtered, and the filtrates were collected in pre-labeled containers according to the experimental matrix. The procedure was repeated for all 29 conditions as specified by the design. The residual urea concentration in each filtrate was determined by titrimetric analysis following a modified Kjeldahl method. The residual material obtained after filtration was designated as Modified Ball Clay After Adsorption (MBCAA) for subsequent characterization.

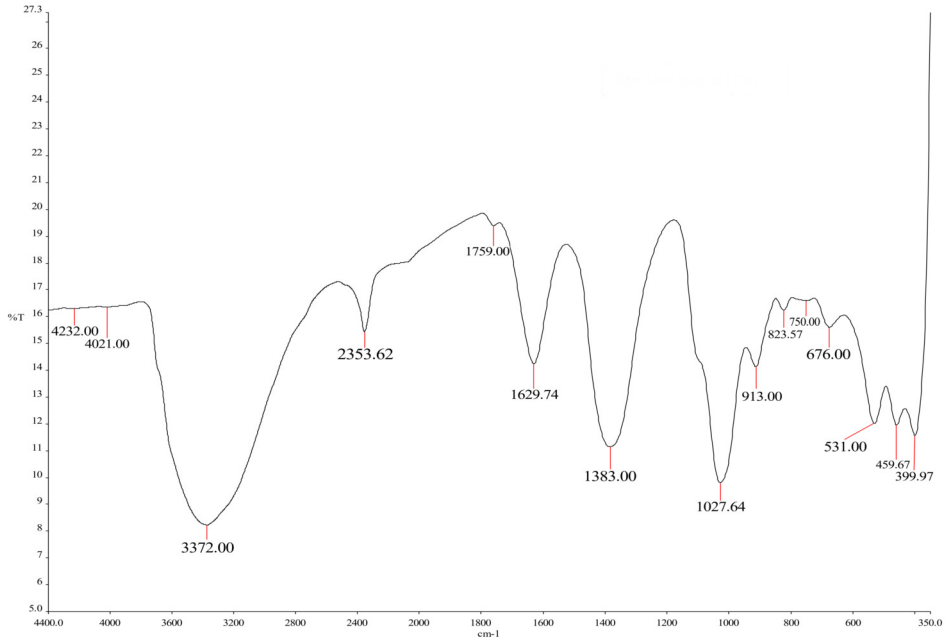


Figure 3. FTIR spectrum for non-modified ball clay after adsorption.

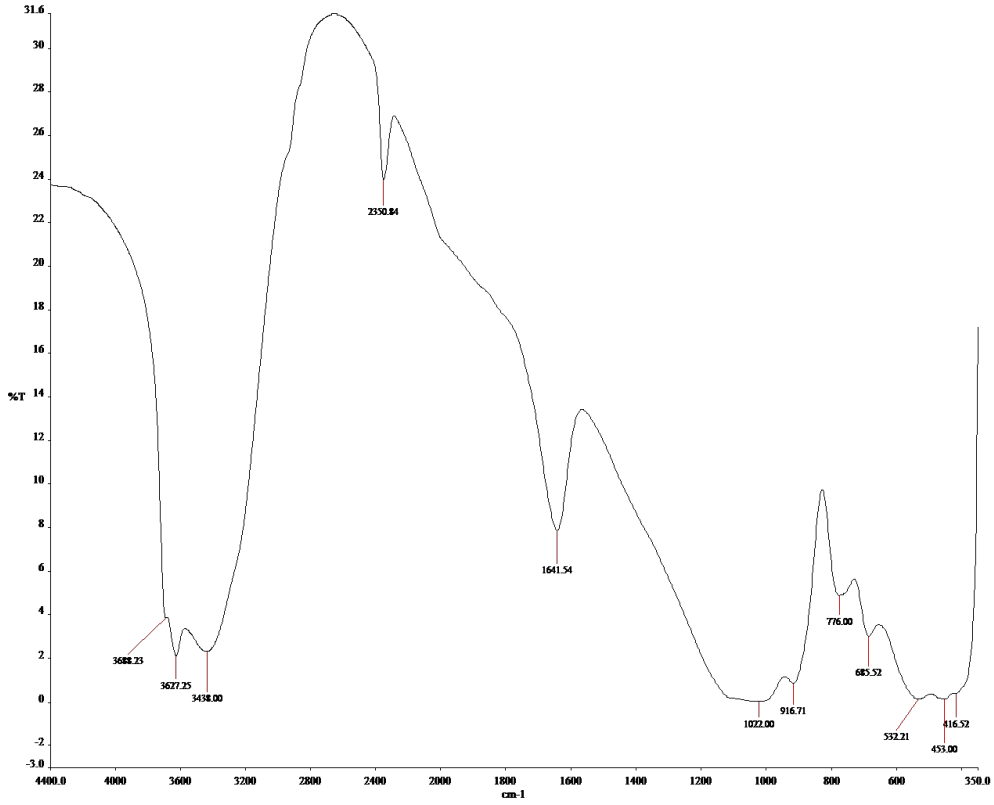


Figure 4. FTIR spectrum for modified ball clay before adsorption.

2.5. Determination of urea using modified Kjeldahl method

To 10 mL of the sample filtrate in a 500 mL Kjeldahl digestion flask, 15 mL of a mixture of salicylic acid and H_2SO_4 was added. The flask was shaken thoroughly and allowed to stand overnight. Next, 0.5 g of $Na_2SO_4.5H_2O$ was added, and the contents were heated gently until the frosting ceased. The flask was then allowed to cool. A catalyst mixture of copper sulfate and potassium sulfate (2 g) was added, and the sample was digested for 3 hours at 380°C. After digestion, the sample was cooled and transferred

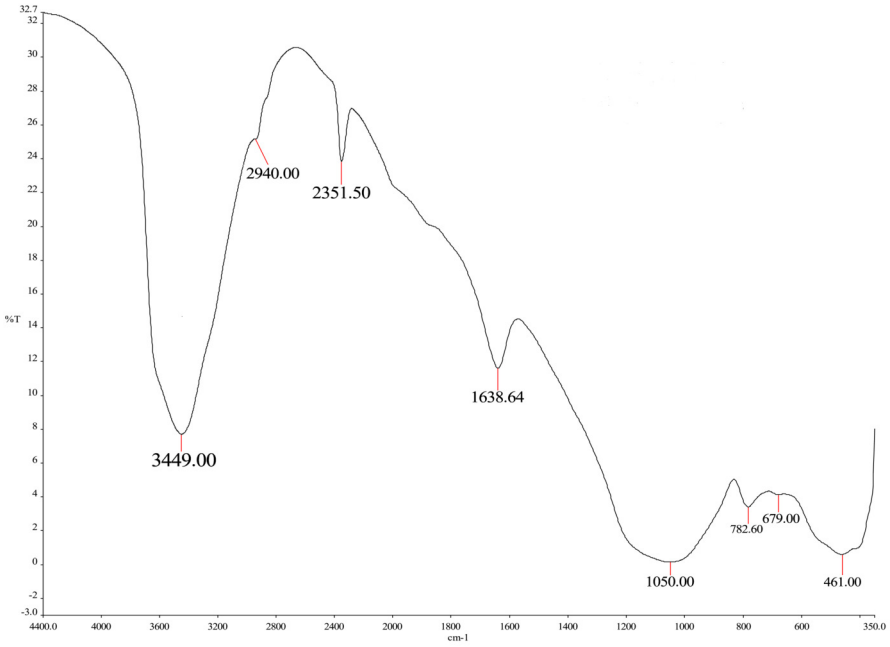


Figure 5. FTIR spectrum for modified ball clay after adsorption.

to a 100 mL volumetric flask, with the volume adjusted to the mark using distilled water. Twenty millilitres (20 mL) of 2% boric acid solution was measured into a 100 mL conical flask and placed at the bottom of the condenser of the Kjeldahl distillation setup. After adding 3 to 5 drops of mixed indicators, 10 mL of the digest and 10 mL of 10N NaOH were added to the distillation flask to liberate the ammoniacal nitrogen. The mixture was then distilled, and the distillate was collected in the conical flask until the volume reached approximately 50 mL (indicated by a green color). The solution was then titrated with 0.025N H_2SO_4 from a green to a purple endpoint. The same procedure was repeated without the analyte of interest to serve as a blank correction. The ammoniacal nitrogen (NH_4-N) and urea content were estimated using equations (1) and (2), respectively, where T is the sample titration value, B is the blank titration value and N is the molarity of the base

$$\text{Ammonical-N (\%)} = \frac{0.014 \times (T - B) \times N \times \text{Vol of Digest} \times 100}{\text{Volume of sample} \times \text{Aliquot}}. \tag{1}$$

Urea is obtained by the following relations:

$$\text{Urea (\%)} = \text{NH}_4\text{-N} \times 2.14\,,$$

and

$$\text{Urea (mg/L)} = \frac{\text{NH}_4\text{-N} \times 2.14}{10^4}. \tag{2}$$

2.6. Data analysis

The adsorption capacity (qe) and adsorptive removal efficiency (Re) were calculated using the concentration difference between the initial concentration and the equilibrium concentration displayed in equations (3) and (4). The rate of urea removal was estimated by dividing the amount of urea adsorbed by the respective contact time shown in equation (5), where C_o is the initial concentration of urea, C_e is the equilibrium concentration of urea, M is the mass of adsorbent (ball clay), V is volume of the solution and Re is the adsorptive removal efficiency as adopted in Ref. [19].

$$\text{Adsorption capacity } (q_e) = \frac{(C_o - C_e)}{M} \times V, \tag{3}$$

$$\text{Removal efficiency } (R_e) = \frac{(C_o - C_e)}{C_o} \times 100, \tag{4}$$

and

$$\text{Rate of adsorption} = \frac{(C_o - C_e)}{t}. \tag{5}$$

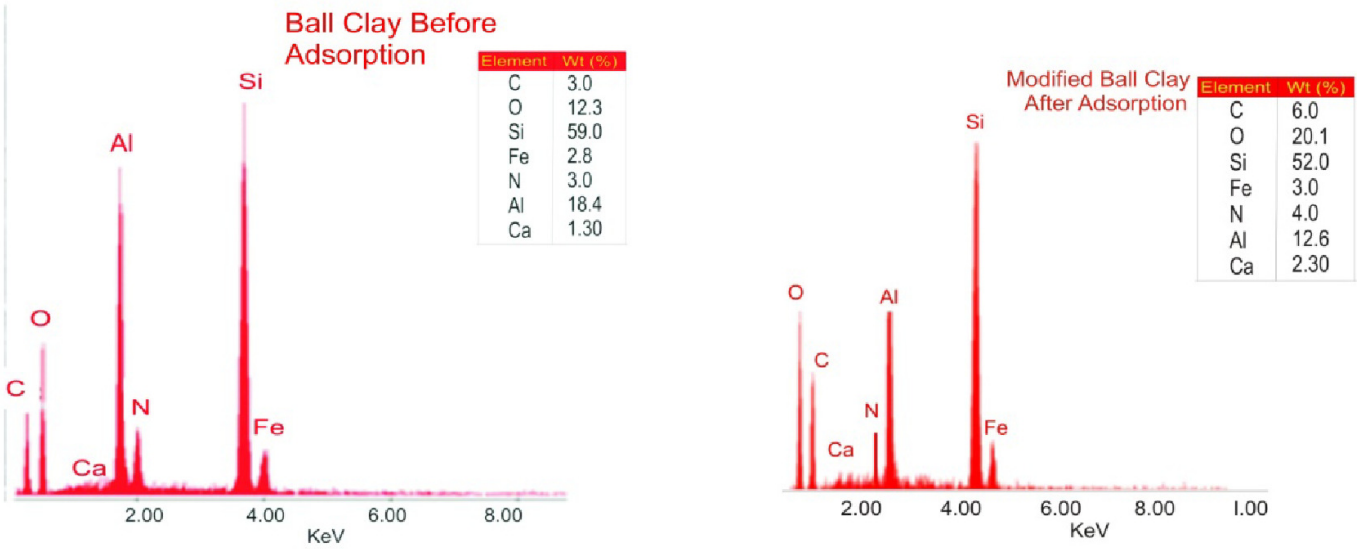


Figure 6. EDX spectrum of ball clay before and after adsorption.

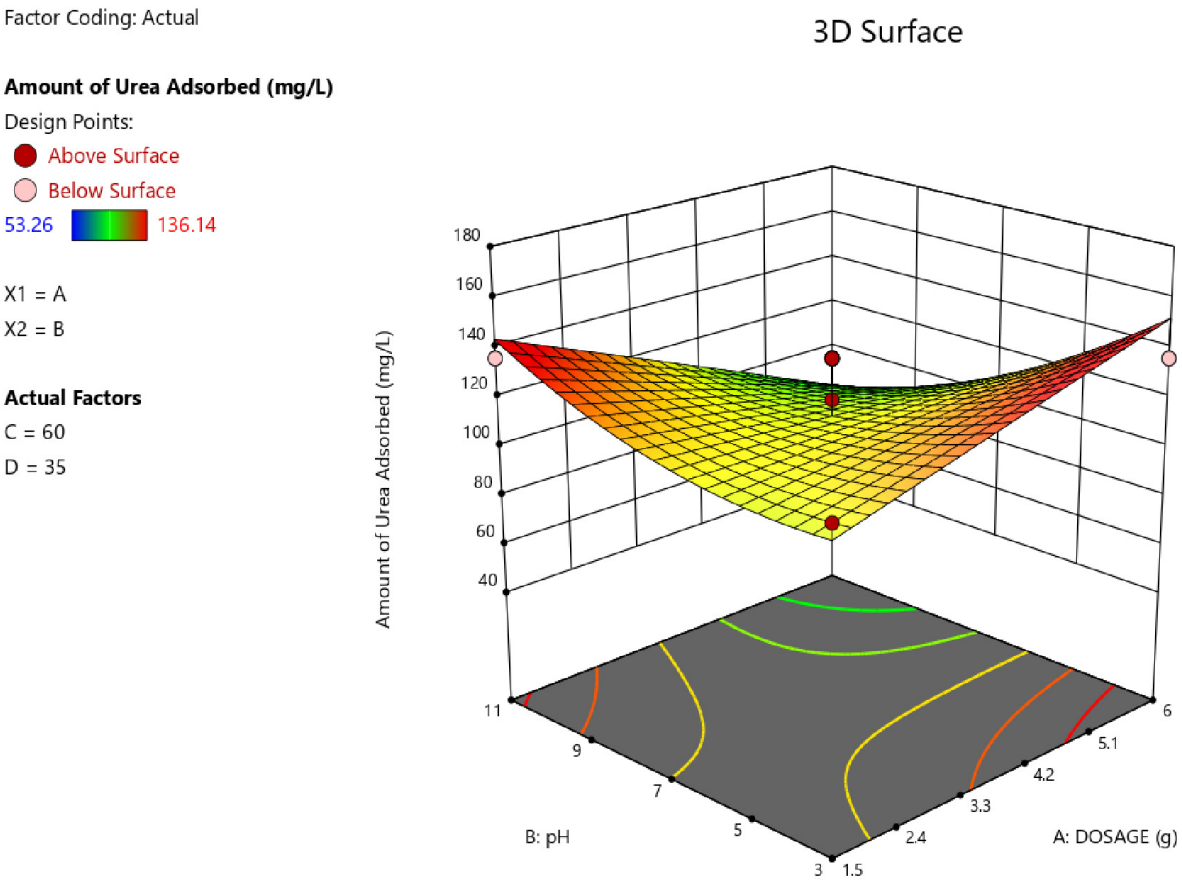


Figure 7. 3D graph for adsorptive removal of urea relative to pH and adsorbent.

Table 1. FT-IR analysis of adsorbent.

Frequency (cm^{-1})	Functional groups	NMBC	MBC	MBCAA	Assignment
4000–3000	Hydroxyl	3449.00	3688.23	3372.00	O–H vibrations of water molecules
2999–1950	Aliphatic acid	2940.00	2350.53	2353.62	C–H bond symmetry stretching
1750–1735	Saturated aliphatic			1750.00	–C=O vibration
1650–1580	Primary amine	1638.64	1641.54	1629.74	N–H bending vibration
1250–1020	Amine			1027	–C–N vibrations
1200–1000	Silicate	1050.00	1022.00	1027.64	Si–O or Al–O stretching
950–750	Silicate or aluminate		916.71	915.00	Si–O–Si and Al–OH bending

3. Results and discussion

The adsorptive removal of urea in agricultural encompasses several stages. Initially, the ball clay was characterized to assess its surface properties and potential for urea adsorption. The agricultural effluent was collected and prepared for the adsorption experiments. The effects of various factors, such as the initial urea concentration, pH of the solution, and temperature, were examined using RSM design. Through systematic experimentation, we explore the interactions between these variables to identify the most favourable conditions for effective urea removal [20, 21].

3.1. Characterization of acid modified ball clay

To determine the surface morphology of the adsorbent, a scanning electron microscope (JEOL JSM 7600F) was employed and the micrograph at 100 µm magnification shown in Figure 1. The surface appears rough with irregular, flaky, and loosely packed particles. The texture is uneven, with noticeable porosity and some agglomeration, indicating a natural, unaltered surface structure before adsorption. After urea adsorption, the surface exhibits a more aggregated and compacted appearance. The particles seem to be coated or covered with urea molecules, resulting in a smoother and less porous surface. The surface texture appears denser and less flaky compared to the un-adsorbed state [22]. The presence of compact tubular crystals, pores, and mono-disperse particle sizes is indicative of an increased number of surface active sites on the adsorbent [23].

Figure 2 presents the Transmission Electron Microscopy (TEM) micrographs of the modified ball clay before and after adsorption at 100 nm. The images reveal the presence of measurable particles within the size range of 1.22 to 5.52 nm, which are roughly spherical or irregular in shape and are randomly dispersed. This dispersion influences the surface area and reactivity of the material. After adsorption, the number of visible measurable particles approximately doubled, with sizes ranging from 1.39 nm to 7.83 nm. The particles appear roughly spherical or irregular in shape, indicating that they largely maintain their size and shape after adsorption. However, the variation in uniformity suggests some degree of heterogeneity, further confirming possible interactions between the ball clay and the adsorbates in the agricultural effluents. This is also evidenced by the presence of particle clusters and aggregations [24].

The FTIR spectrum is essential for identifying surface functional groups, which play a significant role in the adsorption mechanism and capacity [25, 26]. Good adsorbents possess specific properties such as large pores, the availability of oxygen, hydrogen content, and hydroxyl groups [25]. The FTIR analysis was conducted using the KBr disk method [19, 27]. The FTIR spectrum of the non modified ball clay (NMBC) displayed in Figure 3 showed a hydroxyl group peak at 3372 cm^{-1}. After modification with sulfuric acid to remove organic impurities, additional bands were observed at 3688.23, 3627.25, and 3438.00 cm^{-1} as shown in Figure 4, which are associated with out-of-plane vibrations characteristic of well-ordered kaolinite [8, 28]. Furthermore, peaks at 916.71 cm^{-1} (for MBC) and 915 cm^{-1} (for MBCAA) are attributed to Si–O–Si and Al–OH bending vibrations, which are typical of pure kaolinite within the 750–950 cm^{-1} range. Si–O or Al–O stretching vibrations within 1000–1200 cm^{-1} were observed across all adsorbents. The band at 3688.23 cm^{-1}, corresponding to O–H vibrations of water molecules, was noted within the range of 3622–3682 cm^{-1} in the modified clay, indicating the presence of active surface sites capable of interacting with the adsorbate (urea).

In Figure 5, the FTIR spectrum after urea adsorption shows a peak at 1629.74 cm^{-1}, suggesting N–H bending vibrations of a primary amine. Additionally, a less intense peak at 1750 cm^{-1} likely corresponds to the $C = O$ vibration associated with the urea molecule. The band at 1027 cm^{-1} falls within the 1250–1020 cm^{-1} range, indicative of C–N stretching vibrations in urea. The presence of these functional groups suggests that urea molecules can adhere to the adsorbent surface through interactions involving these functional groups.

Figure 6 displays the EDX spectrum for the ball clay, before and after adsorption unveiling the presence of C, O, Al, Si, N, Fe, and Ca. The elemental composition by weight of before adsorption was in the order: Si (59.0%) > Al (18.4%) > O (12.3%) > N (3.0%) = C (3.0%) > Fe (2.8%) > Ca (1.3%). While after adsorption the elemental composition by weight was in the order: Si (52.0%) > O (20.1%) > Al (12.6%) > C (6.0%) = N (4.0%) > Fe (3.0%) > Ca (2.3%). This revealed an increment in the elemental composition of urea such as carbon, nitrogen, oxygen content of the adsorbent after adsorption process. The abundance of Si and Al in the adsorbent is in agreement with the records in a number of scientific literatures capturing the composition of ball clay to be kaolinitic clays with chemical formula ($Al_2O_3.2SiO_2.2H_2O$) consisting of 20 - 80% kaolinite, 10 - 30% mica, 6 - 65% quartz, as well as organic matter trances [8, 9, 29].

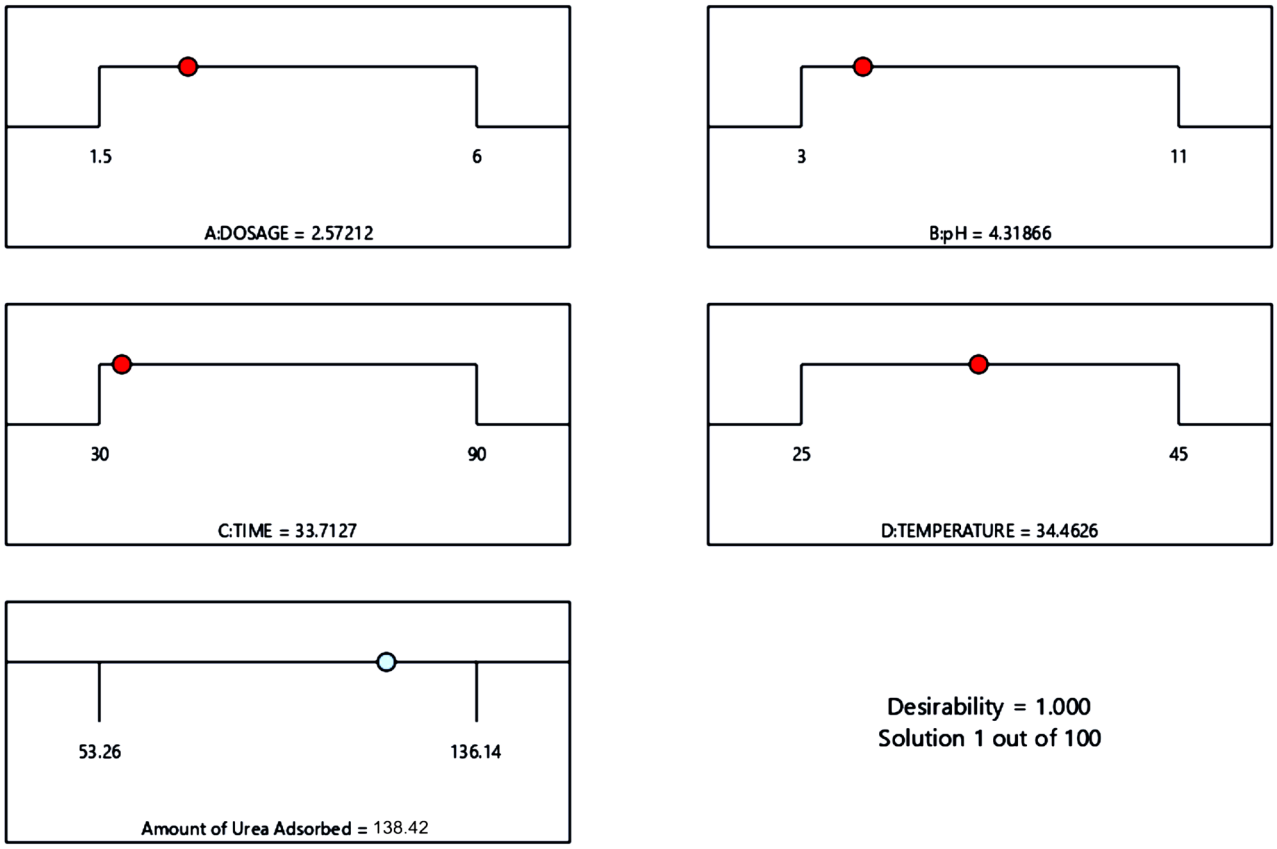


Figure 8. Desirability ramp for optimization.

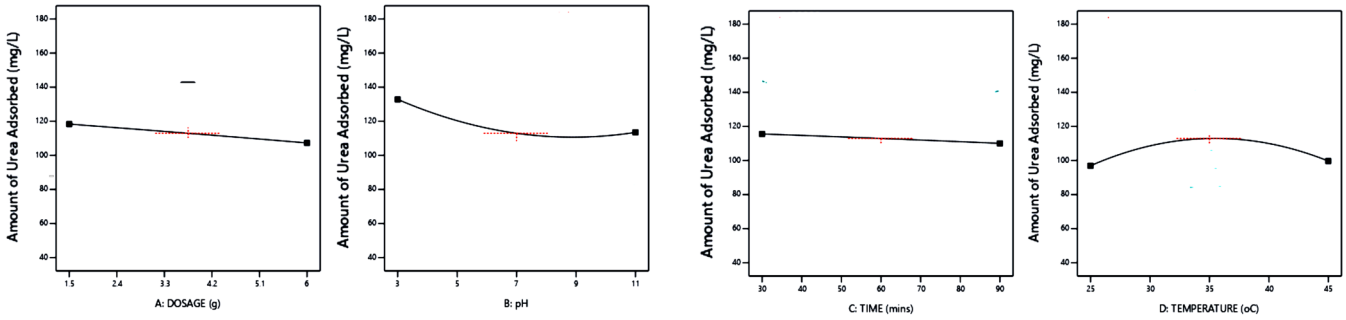


Figure 9. Effect of dosage, temperature, contact time and pH on urea adsorption.

3.2. *Batch adsorption experiments*

Table 2 indicates the equilibrium concentration of urea in agricultural effluents subject to variable temperature, dosage, time and pH. This was carried out by varying the factors in each run for up to 29 runs in order to obtain the best matching factors that attain the optimum adsorption of urea in the agricultural effluent with the highest adsorption of urea concentration. Out of the 29 experimental runs for the adsorptive removal of urea experiment 13 recorded the optimum, 136.15 mg/L urea removal (89.14% removal efficiency) with the removal rate of 4.53 and 4.53 min^{-1} respectively. However, experiment 13 (dosage = 3.75g, pH=3, time = 30 minutes and temperature = 35°C) as well as the best economy of adsorbent use with adsorption capacity (1815.3 mg/g). The 89.14% urea removal efficiency obtained in this study is however less than the 99.23% highest adsorptive removal by thermal activated ball clay and sepiolite composite (at pH = 7, temperature = 25°C, dosage = 0.6 g and time = 60 minutes) as well as the 93.23% of non-activated ball clay and sepiolite composite (at pH = 11, temperature = 35°C, dosage = 0.6 g and time = 60 minutes) reported in Ref

Table 2. Amount of urea adsorbed, adsorption efficiency and rate.

Exp. Run	BCD (g)	pH	Time (min)	Temp (°C)	AUA (mg/L)	Q_e (mg/g)	R_e (%)	R (min^{-1})
1	1.50	11	60	35	134.86	4495.3	88.29	2.24
2	3.75	11	30	35	119.53	1593.7	78.26	3.98
3	3.75	7	60	35	86.43	1152.4	56.59	1.44
4	3.75	7	60	35	135.42	1805.6	88.66	2.25
5	3.75	7	60	35	135.18	1802.4	88.50	2.25
6	1.50	7	60	45	135.79	4526.3	88.90	2.26
7	3.75	11	60	25	119.53	1593.7	78.26	1.99
8	3.75	3	60	25	135.61	1808.1	88.79	2.26
9	3.75	7	90	45	53.26	710.1	34.87	0.59
10	6.00	7	30	35	136.15	1120.9	89.14	4.53
11	6.00	3	60	35	136.15	1134.5	89.14	2.26
12	6.00	7	90	35	86.33	719.4	56.52	0.95
13	3.75*	3*	30*	35*	136.14*	1815.3*	89.14*	4.53*
14	3.75	7	60	35	119.42	1592.2	78.19	1.99
15	3.75	7	30	25	86.33	1151.0	56.52	2.87
16	3.75	11	90	35	86.41	1152.1	56.57	0.96
17	1.50	7	30	35	119.58	3986.0	78.29	3.98
18	3.75	11	60	45	86.61	1154.8	56.70	1.44
19	3.75	7	30	45	86.41	1152.1	56.57	2.88
20	3.75	7	90	25	119.58	1594.4	78.29	1.32
21	1.50	7	90	35	135.74	4524.6	88.87	1.50
22	1.50	3	60	35	119.46	3982.0	78.21	1.99
23	6.00	7	60	45	133.75	1114.5	87.57	2.22
24	3.75	3	60	45	119.76	1596.8	78.41	1.99
25	1.50	7	60	25	53.23	1774.3	34.85	0.88
26	6.00	11	60	35	53.10	442.5	34.76	0.88
27	6.00	7	60	25	86.49	720.7	56.62	1.44
28	3.75	7	60	35	86.41	1152.1	56.57	1.44
29	3.75	3	90	35	119.41	1592.1	78.18	1.32

BCD = Ball clay dosage; AUA = Amount of urea adsorbed; Q_e = Equilibrium adsorption capacity; R_e = Removal efficiency; R = Desorption rate; * = Optimum condition.

[9].

3.3. Optimization of urea adsorption

Figure 7 presents the 3D surface plots generated from the Response Surface Methodology (RSM) model, illustrating the combined effects of pH, adsorbent dosage, temperature, and contact time on urea adsorption by the acid-modified ball clay. These plots depict how each factor interacts to influence the adsorption capacity within the investigated design space. Based on the numerical optimization performed using Design-Expert software, the optimal conditions for maximum urea removal, as shown in Figure 8, were identified as: pH 4.31, adsorbent dosage 2.57 g, temperature 34.46°C, and contact time 33.71 minutes. Under these conditions, the model predicted an adsorption removal of 138.42 mg/L and a removal efficiency of 91.6%, with a desirability index of 1.000, indicating that the software identified the best possible combination of factors within the experimental domain. Experimentally, a run conducted under these optimized conditions produced a urea concentration of 136.14 mg/L and a removal efficiency of 89.8%, closely aligning with the model prediction and thereby validating the reliability of the optimization process.

The least adsorption observed within the studied range was 53.26 mg/g, occurring under conditions far from the statistical optimum (high pH and low dosage). To assess the adequacy of the model, the quadratic regression equation generated by Design-Expert is provided in equation (6).

$$\begin{aligned} Y = {} & -297.82743 + 44.70883\,D - 1.51383\,P + 2.29812\,T + 15.81175\,\mathrm{Temp} \\ & - 2.76222\,(DP) - 0.245519\,(DT) - 0.368333\,(D\,\mathrm{Temp}) \\ & + 0.069000\,(PT) - 0.103813\,(P\,\mathrm{Temp}) - 0.055267\,(T\,\mathrm{Temp}) \\ & - 0.027671\,D^2 + 0.639135\,P^2 - 0.000151\,T^2 - 0.146426\,\mathrm{Temp}^2, \end{aligned} \tag{6}$$

where Y is the amount of urea adsorbed, D is the dosage, P is the pH, T is the time, and Temp is the temperature. The model demonstrated strong statistical significance, with an R^2 of 0.982, an adjusted R^2 of 0.971, and a predicted R^2 of 0.953, indicating excellent agreement between predicted and actual responses. Model validity was further confirmed through residual diagnostics, which showed no severe outliers or systematic patterns, supporting the robustness of the quadratic model for predicting adsorption behavior. Overall, the 3D surface plots and statistical analyses collectively demonstrate that lower pH, moderate adsorbent dosage, elevated temperature, and longer contact time synergistically enhance urea adsorption. The optimal combination identified by the RSM model effectively maximizes the adsorption capacity of the acid-modified ball clay [13].

3.4. Effect of adsorbent dosage, temperature, contact time and pH on urea adsorption

Effect of adsorbent dosage, temperature, contact time and pH on urea adsorption was carried out to understand trends and matching conditions for the optimum removal of urea by MBC. The effect of adsorbent dosage, demonstrated in Figure 9 for MBC. As the amount of adsorbent increases from 1.5 g to 6 g, the removal of urea decreases. When the amount of adsorbent increases, adsorbent particles tend to aggregate or cluster together, thereby reducing the effective surface area available for adsorption. This aggregation diminishes the overall adsorption capacity per unit mass [30]. The effect of pH on urea adsorption showed that the optimum removal was achieved at pH 3, likely due to increased electrostatic attraction between the adsorbate and the adsorbent [31]. Conversely, as the pH approached alkaline conditions at pH 11, a decrease in adsorption was observed, probably due to repulsion between the negatively charged surfaces of the adsorbent and the adsorbate, as the negative charges on the surface increase [32].

The impact of contact time on urea adsorption indicated that the maximum removal was achieved within 30 minutes. Beyond this period, a decline in adsorption capacity was recorded. This trend is likely due to the initial availability of adsorption sites, which become progressively saturated over time [19, 33]. Regarding the effect of temperature, the maximum urea adsorption occurred at an optimal temperature of 35°C. The data showed that urea removal increased with rising temperature up to 35°C before declining, suggesting that preferential adsorption occurs at lower temperatures. Elevated temperatures may increase entropy by enhancing the mobility of adsorbate molecules, thereby reducing adsorption efficiency [34].

4. Conclusion

Acid-modified ball clay exhibits excellent physicochemical properties as an adsorbent and effectively removes urea from wastewater, achieving a removal efficiency of 89.14% at a rate of 4.53 mg/L·min^{-1} and a maximum removal capacity of 1815.3 mg/g when applied to agricultural effluent. The optimal conditions for urea removal were found to be at pH 3, a temperature of 35°C, an acid-modified ball clay dosage of 3.75 g, and a contact time of 30 minutes. The experimentally obtained removal efficiency closely aligns with the prediction from the Response Surface Methodology (RSM), which estimated a removal of 91.6% with a desirability index of 1.000, thereby confirming the reliability of the optimization process. Further research is recommended to explore adsorption isotherms and kinetic models to gain a deeper understanding of the removal mechanism and to enhance the practical applicability of this adsorbent.

Data availability

The datasets generated and analyzed during the current study are available from the corresponding author on reasonable request.

References

[1] M. Gogoi, P. Bhattacharya, S. K. Sen, I. Mukherjee, S. Bhushan & S. R. Chaudhuri, "Aquaculture effluent treatment with ammonia remover *Bacillus albus* (ASSF01)", Journal of Environmental Chemical Engineering **9** (2021) 105697. https://doi.org/10.1016/j.jece.2021.105697.

[2] W. Dilieka, B. Bipai, P. Lokesh, A. Padhye, L. Rachmani, W. James, S. R. Gretel & B. Saeid, "A critical review on current urea removal technologies from water: an approach for pollution prevention and resource recovery", Separation and Purification Technology **314** (2023) 123652. https://doi.org/10.1016/j.seppur.2023.123652.

[3] G. Faye, W. Bekele & N. Fernandez, "Removal of nitrate ion from aqueous solution by modified Ethiopian bentonite clay", International Journal of Research in Pharmacy and Chemistry **4** (2014) 201. https://www.ijrpc.com/files/27-453.pdf.

[4] J. W. Joseph & G. M. Ganga, "A review of the latest in phosphorus fertilizer technology: possibilities and pragmatism", Journal of Environmental Quality **48** (2019) 1313. https://doi.org/10.2134/jeq2019.02.0067.

[5] E. A. Yerima, E. A. Kamba, G. O. Egah, S. P. Maaji, A. I. Ibrahim & S. Zulkifli, "Evaluation of quality index of borehole water in Marmara and New Site communities of Wukari, Nigeria", University of Management and Technology Science Journal **1** (2022) 121. https://doi.org/10.56919/usci.1122.015.

[6] I. V. Zadinelo, H. J. Alves, A. Moesch, L. M. S. Colpini, L. C. Rosa da Silva & L. D. Santos, "Influence of chemical composition of smectites on the removal of ammonium ions from aquaculture effluents", Journal of Materials Science **50** (2015) 1875. https://doi.org/10.1007/s10853-014-8749-3.

[7] E. A. Yerima, E. Ogwuche, C. I. Ndubueze, K. A. Muhammed & J. D. Habila, "Photocatalytic degradation of acid blue 25 dye in wastewater by zinc oxide nanoparticles", Trends in Ecological and Indoor Environment Engineering **2** (2024) 56. https://www.researchgate.net/publication/380406646.

[8] K. A. Galos, "Composition and ceramic properties of ball clays for porcelain stoneware tiles manufacture in Poland", Applied Clay Science **51** (2011) 85. https://doi.org/10.1016/j.clay.2010.11.004.

[9] E. A. Yerima, H. Ataitiya, B. N. Hikon, G. O. Egah, S. P. Maaji, A. I. Ibrahim, C. O. Ogar & Z. S. Samuel, "Synergistic adsorptive removal of urea from agricultural effluents using ball clay and sepiolite composite", Journal of Biotechnology Research **10** (2023) 19. https://doi.org/10.32861/jbr.101.9.19.

[10] R. L. Naylor, R. J. Goldburg, J. H. Primavera, N. Kautsky, M. C. M. Beveridge, J. Clay, C. Folke, J. Lubchenco, H. Mooney & M. Troell, "Effect of aquaculture on world fish supplies", Nature **405** (2000) 1024. https://doi.org/10.1038/35016500.

[11] I. Geremia, J. A. W. van Jong, C. F. van Nostrum, W. E. Hennink, K. G. F. Gerritsen & D. Stamatialis, "New mixed matrix membrane for the removal of urea from dialysate solution", Separation and Purification Technology **277** (2021) 119408. https://doi.org/10.1016/j.seppur.2021.119408.

[12] J. O. Ighalo, S. Rangabhashiyam, K. Dulta, C. T. Umeh, K. O. Iwuozor, C. O. Aniagor, S. O. Eshiemogie, F. U. Iwuchukwu & C. A. Igwegbe, "Recent advances in hydrochar application for the adsorptive removal of wastewater pollutants", Chemical Engineering Research and Design **184** (2022) 456. https://doi.org/10.1016/j.cherd.2022.06.028.

[13] D. Abutu, B. O. Aderemi, A. O. Ameh, H. W. Yussof, J. Gbonhinbor, B. Money, F. Nyah, C. Umunnawuike, P. I. Nwaichi & A. Agi, "Optimization of ethanol fermentation in a bubble column bioreactor using response surface methodology with ferric oxide nanoparticle-modified supports", in *Proceedings of the SPE Nigeria Annual International Conference and Exhibition*, August 4, Society of Petroleum Engineers, 2025. https://doi.org/10.2118/228638-MS.

[14] D. Abutu, B. O. Aderemi, A. O. Ameh, H. W. Yussof, E. A. Yerima & A. Agi, "Integrated experimental and numerical study of a bubble column bioreactor with immobilized S. cerevisiae for ethanol production in non-Newtonian fermentation broth", Chemical Engineering Communications (2025) 19. https://doi.org/10.1080/00986445.2025.2572738.

[15] D. Schwante, A. C. Goncalves Jr, G. F. Coelho, M. A. Campagnolo, D. C. T. Dragunski, C. R. Tarley, A. J. Miola & E. A. V. Leismann, "Chemical modification of cassava peel as adsorbent material for metal ions from wastewater", Journal of Chemistry **2016** (2016) 3694174. http://dx.doi.org/10.1155/2016/3694174.

[16] T. N. M. Ngo, M. N. Nguyen, L. N. H. Cao Luu, T. B. Q. Tran, V. N. H. Nguyen & N. P. L. Tran, "Study of the activation of Truc Thon ball clay by acids", CTU Journal of Innovation and Sustainable Development **15** (2023) 102. http://dx.doi.org/10.22144/ctujoisd.2023.054.

[17] B. Money, A. B. Qurratu, S. Mahat, N. Ismail, M. R. Hassan, D. Abutu & A. A. Augustine, "Clay-based geopolymers cement for oil wells: a bibliometric analysis and literature review", in *Clay Science – bridging geology and physical chemistry*, IntechOpen, London, United Kingdom, 2025. https://doi.org/10.5772/intechopen.1011806.

[18] D. Abutu, B. O. Aderemi, A. O. Ameh, H. W. Yussof & A. Agi, "Nano-enhanced biocarriers: ferric oxide-modified chitosan and calcium alginate beads for improved fermentation efficiency and reusability in a bubble column bioreactor", Biotechnology Letters **47** (2025) 70. https://doi.org/10.1007/s10529-025-03611-6.

[19] E. A. Yerima, S. P. Maaji, D. Abutu, H. Ataitiya, O. Ekirigwe, S. N. Johnson & A. Shem, "Adoption of response surface methodology in the optimization of ammonia removal from aquaculture effluent using thermal activated and non-activated ball clay", IOSR Journal of Environmental Science, Toxicology and Food Technology **18** (2024) 9. https://www.iosrjournals.org/iosr-jestft/papers/Vol18-Issue2/Ser-2/A1802020109.pdf.

[20] A. K. Agarwal & M. S. Kadu, "Kinetics study on the adsorption of Ni^{2+} ions onto fly ash", Journal of Chemical Technology and Metallurgy **50** (2015) 605. https://www.researchgate.net/publication/282572056.

[21] T. P. Araújo, L. S. Brighenti, H. B. Santos, A. H. F. Castro & R. G. Thomé, "Toxicity of nitrogen compounds in fish influenced by physico-chemical water parameters: a review", Research and Society Development **10** (2021) e359101119779. https://doi.org/10.33448/rsd-v10i11.19779.

[22] M. Naswir, S. A. Rachman, M. Marsi & S. Salni, "Characterization of bentonite by X-ray diffraction and scanning electron microscopy with energy dispersive spectroscopy and use to increase pH and color removal, Fe and organic substances in peat water", Journal of Clean Energy Technology **1** (2013) 317. https://doi.org/10.7763/JOCET.2013.V1.71.

[23] A. S. Ahmed, A. M. Tantawy, M. E. Abdallah & I. M. Qassim, "Characterization and application of kaolinite clay as solid phase extractor for removal of copper ions from environmental water samples", International Journal of Advanced Research **3** (2015) 21. https://www.journalijar.com/uploads/2015/03/835_IJAR-5066.pdf.

[24] M. R. Abass, E. H. El-Masry & A. B. Ibrahim, "Preparation, characterization, and applications of polyacrylonitrile/ball clay nanocomposite synthesized by gamma radiation", Environmental Geochemistry and Health **43** (2021) 3188. https://doi.org/10.1007/s10653-021-00813-5.

[25] D. Kibami, C. Pongener, K. S. Rao & D. Sinha, "Preparation and characterization of activated carbon from *Fagopyrum esculentum* Moench by HNO_3 and H_3PO_4 chemical activation", Der Chemica Sinica **5** (2014) 55. https://paperzz.com/doc/9057471/preparation-and-characterization-of-activated-carbon-from.

[26] M. Moradi, A. Dehpahlavan, R. Kalantary, A. Ameri, M. Farzadkia & H. Izanoo, "Application of modified bentonite using sulfuric acid for the removal of hexavalent chromium from aqueous solutions", Environmental Health Engineering and Management Journal **2** (2015) 106. https://applications.emro.who.int/imemrf/Environ_Health_Eng_Manag_J/Environ_Health_Eng_Manag_J_2015_2_3_99_106.pdf.

[27] G. Dal Poggetto, A. D'Angelo, I. Blanco, S. Piccolella, C. Leonelli & M. Catauro, "FTIR study, thermal analysis, and evaluation of the antibacterial activity of a MK-geopolymer mortar using glass waste as fine aggregate", Polymers **13** (2021) 2970. https://doi.org/10.3390/polym13172970.

[28] E. Balan, A. M. Saitta, F. Mauri & G. Galas, "First principles modeling of the infrared spectrum of kaolinite", American Mineralogist **86** (2001) 1330. https://doi.org/10.2138/am-2001-11-1201.

[29] I. R. Wilson, "The constitution, evaluation and ceramic properties of ball clays", Cerâmica **44** (1998) 288. https://doi.org/10.1590/S0366-69131998000400002.

[30] M. Molebatsi, B. Nkoane, N. Keroletswe, S. Chigome & M. T. Kabomo, "The use of biosorbents in water treatment", Environment **12** (2025) 302. https://doi.org/10.3390/environments12090302.

[31] F. Bolat, S. Govori, A. Haziri, S. Spahiu & F. Faiku, "Used tea waste adsorption for removal of phenol from synthetic and Kosovo industrial wastewater", Journal of Marine Science and Application **5** (2010) 67. https://www.researchgate.net/publication/309994915.

[32] A. Denizli, G. Ozkan & M. Ucar, "Removal of chlorophenols from aquatic systems with dye affinity microbeads", Separation and Purification Technology **24** (2001) 262. https://doi.org/10.1016/S1383-5866(01)00129-0.

[33] A. A. Adeyemo, I. O. Adeoye & O. S. Bello, "Adsorption of dyes using different types of clay: a review", Applied Water Science **7** (2017) 568. https://doi.org/10.1007/s13201-015-0322-y.

[34] B. Riebe & C. Bunnenberg, "Influence of temperature pre-treatment and high molar saline solutions on the adsorption capacity of organo-clay minerals", Physics and Chemistry of the Earth **32** (2007) 587. https://doi.org/10.1016/j.pce.2006.02.060.